Life Sciences 89 (2011) 609–614

Contents lists available at SciVerse ScienceDirect

Life Sciences

journal homepage: www.elsevier.com/locate/lifescie

Rat liver uncoupling protein 2: Changes induced by a fructose-rich diet

María C. Castro [1], María L. Massa [1], Héctor Del Zotto, Juan J. Gagliardino, Flavio Francini *

CENEXA – Centro de Endocrinología Experimental y Aplicada (UNLP-CONICET LA PLATA, Centro Colaborador OPS/OMS en Diabetes), Facultad de Ciencias Médicas, Calles 60 y 120, 1900 La Plata, Argentina

ARTICLE INFO

Article history:
Received 16 February 2011
Accepted 21 July 2011

Keywords:
Fructose-rich diet
Liver uncoupling protein 2
Peroxisome proliferator-activated receptors regulation
Glycoxidative stress

ABSTRACT

Aim: To evaluate the role of uncoupling protein 2 (UCP2) and peroxisome proliferator-activated receptors (PPARs) in the response of liver to glycoxidative stress triggered by administration of a fructose-rich diet (FRD).
Main methods: We assessed blood glucose in the fasting state and after a glucose load (glucose-oxidase method), serum triglyceride (enzymatic measurement), insulin (radioimmunoassay), alanine aminotransferase (ALT) and aspartate aminotransferase (AST) levels (colorimetric kits) in control and FRD animals. In liver, we measured UCP2, PPARα, PPARδ and PPARγ gene (real-time PCR) and protein (Western blot) expression, fatty acid synthase (FAS) and glycerol-3-phosphate acyltransferase (GPAT) gene expression, as well as triglyceride content.
Key findings: Blood glucose, serum insulin and triglyceride levels, homeostasis model assessment of insulin resistance (HOMA-IR) indexes and impaired glucose tolerance were higher in FRD rats. Whereas UCP2 and PPARδ gene and protein expression increased in these animals; PPARγ levels were lower and those of PPARα remained unchanged. FRD also increased the mRNA expression of PPARδ target genes FAS and GPAT.
Significance: Our results suggest that a) the increased UCP2 gene and protein expression measured in FRD rats could be part of a compensatory mechanism to reduce reactive oxygen species production induced by the fructose overload, and b) PPARs expression participates actively in the regulation of UCP2 expression, and under the metabolic condition tested, PPARδ played a key role. This knowledge would help to better understand the mechanisms involved in liver adaptation to fructose-induced glycoxidative stress, and to develop appropriate prevention strategies in obesity and type 2 diabetes.

Introduction

The prevalence of diabetes increases exponentially worldwide, and it is estimated that by 2025 it will affect 300 million people (King et al., 1998). At the same time, both an increased consumption of unhealthy high calorie diets and a sedentary behavior have been recorded in modern societies (Guthrie and Morton, 2000). The increase in total energy consumption has been accompanied by a shift in the types of nutrients consumed (Putnam and Allshouse, 1999) and some reported evidence suggests that the increased use of fructose-rich syrups and refined carbohydrates has greatly contributed to the current epidemic of obesity and type 2 diabetes (T2DM) (Bray et al., 2004; Gross et al., 2004; Malik et al., 2010). Although the underlying mechanism responsible for the detrimental effects of fructose-rich diets (FRD) is not quite clear, it is known that such diets promote an increase of glycoxidative stress (Busserolles et al., 2002; Girard et al., 2006; Lange et al., 1980; Thirunavukkarasu et al., 2004). In fact, we have previously demonstrated that short-term administration of a FRD to normal rats induces significant changes in many metabolic, endocrine and glycoxidative stress markers (Alzamendi et al., 2009; Francini et al., 2009, 2010; Rebolledo et al., 2008).

Mitochondrial function plays an important role in the glycoxidative process as a source of reactive oxygen species (ROS) produced by the activity of the respiratory chain (Rousset et al., 2004). On the other hand, ROS production actively modulates the mitochondrial membrane potential (Boss et al., 2000): high membrane potential inhibits the flow down of the electron transport chain, with the consequent increase in the half-life of intermediates of this chain capable of reducing O_2 to O_2^-. Further, when little ADP is available for its phosphorylation to ATP, there is a reduction in ATP synthase activity that leads to an increase in mitochondrial membrane potential. Conversely, an overload of nutrients would decrease ATP utilization inhibiting oxygen consumption; this inhibition would increase ROS production, causing oxidative stress (Boss et al., 2000). Skulachev (1998) proposed a regulatory mechanism for this process called "mild" uncoupling, which prevents large increases in mitochondrial membrane potential when ADP is not available, thus reducing ROS production by the respiratory chain. Uncoupling proteins (UCPs), which are mitochondrial transporters of the inner membrane, appear to play a significant role in this antioxidant defense mechanism (Rousset et al., 2004).

In an attempt to provide a deeper insight into the above described mechanism of fructose- induced glycoxidative stress, we studied the

* Corresponding author. Tel.: +54 221 423 6712; fax: +54 221 422 2081.
E-mail address: f_francini@yahoo.com (F. Francini).
[1] These authors contributed equally to this work.

0024-3205/$ – see front matter © 2011 Elsevier Inc. All rights reserved.
doi:10.1016/j.lfs.2011.07.024

possible role of liver UCP2 in the adaptive reaction to such process. For this purpose, we measured the gene expression and protein levels of UCP2 and of known regulators of its expression, namely, peroxisome proliferator-activated receptors (PPARs), in animals fed a FRD.

Materials and methods

Chemicals and drugs

Reagents of the purest available grade were obtained from Sigma Chemical Co. (St. Louis, MO, USA). The anti-rat UCP2 antibody was kindly provided by Dr. Ewa Gurgul-Convey (Medizinische Hochschule Hannover, Hannover, Germany). PPARs antibodies were obtained from Santa Cruz Biotechnology, Inc. (Santa Cruz, California, USA). The secondary antibody (peroxidase-conjugated AffiniPure donkey anti-rabbit IgG) was provided by Dianova (Hamburg, Germany).

Animals

Normal male Wistar rats (150–180 g bw) were maintained in a temperature-controlled room (23 °C) with a fixed 12-h light–dark cycle (06:00–18:00 h). One group of 15 animals had free access to a standard commercial diet and tap water (control, C) while another group received the same diet plus 10% fructose in the drinking water (FRD).

Water intake was measured daily, while individual body weight was recorded once a week. This procedure was replicated 5 times and every sample was run in triplicate.

Twenty-one days after this treatment, blood samples from 4-h fasted animals of both groups were drawn from the retroorbital plexus under light halothane anesthesia and collected into heparinized tubes to measure blood glucose and serum triglyceride and immunoreactive insulin levels. Afterwards, the animals were killed by decapitation and the same portion of liver (median lobe) was removed to perform all the assays.

Animal experiments and handling were performed according to the "Ethical principles and guidelines for experimental animals" (3rd Edition 2005) of the Swiss Academy of Medical Sciences.

Serum measurements

Glucose was measured with the glucose-oxidase GOD-PAP method (Roche Diagnostics, Mannheim, Germany); triglyceride levels were assayed enzymatically with a commercial kit (TG color GPO/PAP AA, Wiener lab, Argentina) implemented in an automated clinical analyzer.

Immunoreactive insulin levels were determined by radioimmunoassay (RIA) (Herbert et al., 1965) using an antibody against rat insulin, rat insulin standard (Linco Research Inc., IN, USA), and highly-purified porcine insulin labeled with ^{125}I (Linde et al., 1980). Serum insulin and fasting blood glucose values were used to estimate insulin resistance with the homeostasis model assessment of insulin resistance (HOMA-IR) index with the formula (Serum insulin μU/ml x fasting blood glucose mM)/22.5 (Matthews et al., 1985).

The serum levels of alanine aminotransferase (ALT) and aspartate aminotransferase (AST) were determined with commercial colorimetric kits (Bio Systems S.A., Costa Brava, 30, Barcelona, Spain).

Glucose tolerance

The day before sacrifice, glucose tolerance was measured in 12 h-fasted rats after i.p. glucose injection (1 g/kg in saline). Blood samples were obtained as explained before at 0, 15, 30, 60 and 120 min under pentobarbital anesthesia (48 mg/kg). Results were expressed as the area under the glucose curve (AUC) in mM/min.

Liver measurements

Assessment of reduced glutathione (GSH) and protein carbonyl groups

Protein carbonyl content was assayed by the procedure of Levine et al. (1990). Liver homogenates were centrifuged and 0.5 ml of the supernatant were mixed with 10 mM 2,4-Dinitrophenylhydrazine (DNPH) in 2 M hydrochloric acid and incubated for 1 h at room temperature; thereafter, the mixture was precipitated with 20% trichloroacetic acid (TCA). The pelleted protein was washed thrice by resuspension in ethanol/ethyl acetate (1:1). Proteins were then solubilized in 6 M guanidine hydrochloride and centrifuged at 16,000 ×*g* for 5 min to remove any trace of insoluble material. The carbonyl content was measured spectrophotometrically at 366 nm. A tissue blank incubated with 2 M HCl without DNPH was included for each sample. Results were expressed as nmol of carbonyl residues/mg protein based on the molar extinction coefficient of 21,000 M^{-1} cm^{-1}. GSH in liver was determined by the method of Ellman (Sedlak and Lindsay, 1968).

Lipid and triglyceride content

Lipid accumulation in the liver of animals from each experimental group was measured (histochemistry) with Sudan Red staining. Briefly, samples were fixed with 5% formalin solution and frozen tissue was cut with a freezing-microtome. Frozen sections (>5 μm) were embedded in 50% ethanol for 1–2 min and then stained for 30 min a room temperature with Sudan Red. Sudan Red solution was prepared as a saturated solution of the dye in a 1:1 (v/v) mixture of 50% ethanol–acetone. After that, the sections were washed 5 min in 50% ethanol in order to remove the excess of dye. The morphological analysis was performed using a Nikon Eclipse 80i light microscope and photography obtained with Nikon digital Sight DS-U1.

Liver triglyceride extraction was performed as described by Schwartz and Wollins (2007) and assayed with a commercial kit, as described for serum measurements.

Total RNA

Total liver RNA from FRD and C rats was isolated using TRIzol Reagent (Gibco-BRL, Rockville, MD, USA) (Chomczynski and Sacchi, 1987). The integrity of the isolated RNA was checked by running it on 1% agarose-formaldehyde gel electrophoresis. Possible contamination with protein or phenol was tested by measuring the 260/280 nm absorbance ratio, while DNA contamination was avoided using DNase I digestion (Gibco-BRL). Reverse transcription-PCR was performed using the SuperScript III (Gibco-BRL) and total RNA (50 ng) from FRD and C liver as a template.

Analysis of gene expression by real-time PCR (qPCR)

qPCR was performed with a Mini Opticon Real-Time PCR Detector Separate MJR (BioRad), using SYBR Green I as a fluorescent dye that binds only double-stranded DNA. Ten ng of cDNA were amplified in a 25 μl qPCR reaction mixture containing 0.36 μM of each primer, 3 mM $MgCl_2$, 0.2 mM dNTPs and 0.15 μl Platinum Taq DNA polymerase 6 U/μl (Invitrogen). Samples were first denatured at 95 ° C for 3 min followed by 40 PCR cycles. Each cycle comprised a melting step at 95 ° C for 30 sec, an annealing step at 65 ° C for 30 sec and an extension step at 72 ° C for 45 sec, followed by a final extension at 72 ° C for 10 min. The optimal parameters for the PCR reactions were empirically defined. Each PCR amplification was performed in triplicate.

The oligonucleotide primers (Invitrogen) used are listed in Table 1. All amplicons were designed in a size range of 90 to 250 bp. β-actin was used as housekeeping gene. SYBR Green fluorescence emission was determined after each cycle. The purity and specificity of the amplified PCR products were verified by performing melting curves generated at the end of each PCR. Product length and PCR specificity

Table 1
Sequence of pair of primers used for qPCR.

Gene	GenBank®	Sequences
UCP2	NM_019354	FW 5′-GGTAAAGGTCCGCTTCCAGG-3′ RV 5′-GCAAGGGAGGTCGTCTGTCA-3′
PPARα	NM_013196	FW 5′-CACCCTCTCTCCAGCTTCCA-3′ RV 5′-GCCTTGTCCCCACATATTCG-3′
PPARγ	NM_013124	FW 5′-ATGGAGCCTAAGTTTGAGTTTGCT-3′ RV 5′-GGATGTCCTCGATGGGCTTCA-3′
PPARδ	NM_013141	FW 5′-AACGAGATCAGCGTGCATGTG-3′ RV 5′-TGAGGAAGAGGCTGCTGAAGTT-3′
FAS	M76767.1	FW 5′-GTCTGCAGCTACCCACCCGTG-3′ RV 5′-CTTCTCCAGGGTGGGGACCAG-3′
GPAT	AF021348	FW 5′-GACGAAGCCTTCCGAAGGA-3′ RV 5′-GACGAAGCCTTCCGAAGGA-3′
β-actin	NM_019130	FW 5′-AGAGGGAAATCGTGCGTGAC-3′ RV 5′-CGATAGTGATGACCTGACCGT-3′

Fw, forward (sense) primer; Rv, reverse (antisense) primer.

were further checked by 2% (w/v) agarose gel electrophoresis and ethidium bromide staining. Data are expressed as relative gene expression after normalization to the β-actin housekeeping gene using the *Qgene96* and *LineRegPCR* software, as described elsewhere (Francini et al., 2009).

Western blot analysis

UCP2, PPARα, PPARγ and PPARδ immunodetection was performed using liver homogenates from each experimental group. Protein concentration was quantified by the Bio-Rad protein assay (Bradford, 1976); thereafter, dithiothreitol and bromophenol blue were added to the samples to a final concentration of 100 mM and 0.1%, respectively. Aliquots of homogenates containing 100 μg of whole protein were placed in reducing 12.5% SDS-PAGE and electroblotted to polyvinylidene difluoride membranes. The amount of protein loaded was confirmed by the Bradford method (Bradford, 1976) and the uniformity of protein loading in each lane was assessed by staining the blot with Ponceau S. Nonspecific binding sites of the membranes were blocked by overnight incubation with non-fat dry milk at 4 °C. Enzyme identification and quantification were performed using specific primary antibodies against UCP2 (1:500), PPARα (1:1000), PPARγ (1:1000) and PPARδ (1:1000) overnight. At the end of the incubation period, the membranes were rinsed in phosphate buffered saline (PBS) pH 7.4, and further incubated for 1 h and 15 min with the corresponding secondary antibody (anti-goat IgG biotinyl antibody, 1:1000); at the end of this incubation, the membranes were rinsed in PBS and incubated for 1 h and 15 min with the streptavidin-peroxidase complex (1:2500). For PPARs antibodies, the membranes were incubated in anti-rabbit peroxidase conjugated antibody and later rinsed in PBS. Diaminobenzidine (DAB, Sigma Co.) was used for color development. Finally, the bands were quantified by densitometry using the Gel-Pro Analyser software.

Statistical analysis

Data are expressed as means ± SEM unless specifically stated. Statistical analyses were performed using ANOVA followed by Dunnett's test for multiple comparisons or *t*-test for correlations using the Prism analysis program (Graphpad, San Diego, USA). Differences were considered significant when $P<0.05$.

Results

Body weight and water intake

Comparable body weights were recorded in FRD and C animals after the 3-week study period (290 ± 5 vs. 292 ± 12 g, respectively). FRD animals drank a larger volume of water than C (42.8 ± 2.4 vs. 33.1 ± 3.0 ml/day; $P<0.02$). Conversely, C rats ate a significantly larger amount of solid food than FRD rats (22.1 ± 1.4 vs. 16.5 ± 1.7 g/animal/day; $P<0.001$). Consequently, while the percent daily intake of nutrients (% weight) was different in both experimental groups (C: 45:43:12 carbohydrates: proteins:lipids; FRD: 60:31:9 carbohydrates:proteins:lipids), calorie intake was comparable (C: 63.8 ± 4.9; FRD: 64.8 ± 3.7 kcal/day).

Serum measurements

FRD rats had significantly higher blood glucose and serum insulin and triglyceride concentrations than C rats (Table 2). Although blood glucose levels were higher in FRD animals, they remained within normal range.

The HOMA-IR values demonstrated the existence of an insulin resistance state in FRD rats (Table 2).

Analysis of serum markers of liver function (ALT and AST) showed no differences between groups (Table 2).

Glucose tolerance

Blood glucose AUC values following *i.p.* glucose administration were significantly higher in FRD as compared to C rats (FRD: 4.31 ± 0.5; C: 1.57 ± 0.63 mM/min; $P<0.01$).

Assessment of reduced glutathione (GSH) and protein carbonyl groups

Protein carbonyl content was significantly higher in FRD than in C rats (Fig. 1) while the total content of GSH was significantly lower in FRD animals (Fig. 1).

Liver lipid accumulation and triglyceride content

The histological analysis showed a significant increase of ectopic fat deposition in FRD rat liver compared with C animals (Fig. 2). Supporting these results, triglyceride content was higher in FRD liver samples (756.2 ± 43.1 vs. 549.5 ± 17.6 μg/100 mg tissue; $P<0.001$).

q-PCR

UCP2 and PPARδ gene expression (normalized to β-actin gene) was significantly higher in FRD rats, that of PPARγ was significantly decreased, and PPARα gene expression remained unchanged (Fig. 3A). The expression of PPARδ target genes fatty acid synthase (FAS) and glycerol-3-phosphate acyltransferase (GPAT) also increased significantly in these rats (FAS, 6123.18 ± 825 vs. 2338.33 ± 232; $P<0.005$; GPAT, 1.62 ± 0.28 vs. 0.754 ± 0.25; $P<0.05$).

Western blot analyses

Western blots performed in samples from C and FRD animals using specific anti- UCP2, PPARα, PPARγ and PPARδ antibodies showed single bands compatible with the molecular weight of the corresponding

Table 2
Serum measurements.

	C	FRD
Blood glucose (mM)	7.4 ± 0.2	8.1 ± 0.2*
Serum insulin (ng/ml)	2.3 ± 0.3	4.0 ± 0.5*
Serum triglycerides (mM)	1.0 ± 0.1	1.6 ± 0.1#
HOMA-IR	18.9 ± 1.8	36 ± 3#
ALT (U/L)	42.1 ± 2.7	36.9 ± 1.7
AST (U/L)	130.3 ± 11.1	120.2 ± 11.4

Values are means ± S.E.M. of 5 individual experiments run in triplicate for C and FRD animals.
* $p<0.05$.
\# $p<0.005$.

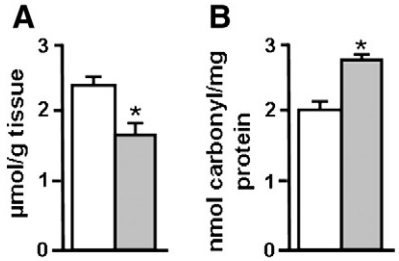

Fig. 1. Assessment of reduced glutathione (GSH) (A) and protein carbonyl groups (B) in C (white bars) and FRD (gray bars) animals. Results are means ± SEM of 5 different experiments run in triplicate. *$P<0.05$.

proteins. The intensity of the specific bands increased as a function of the protein concentration used, supporting the reliability and specificity of the immune measurements (data not shown).

UCP2 protein expression in liver homogenates from FRD animals was significantly higher than that measured in C animals (Fig. 3B and C). While PPARγ protein expression decreased, the one corresponding to PPARδ was significantly enhanced (Fig. 3B and C) and that of PPARα had no changes in FRD compared with C animals.

Discussion

As previously reported, our FRD-fed rats presented insulin resistance, as demonstrated by hyperinsulinemia with normoglycemia and the HOMA-IR index, significantly increased serum triglyceride levels, impaired glucose tolerance and oxidative stress markers (Alzamendi et al., 2009; Francini et al., 2009, 2010; Rebolledo et al., 2008).

The presence of UCP2 has been described in different tissues; however, the lowest level of liver UCP2 expression is attained under basal conditions (Villarroya et al., 2007). Although Kupffer cells are a dominant site of UCP2 expression in adult rat liver (Larrouy et al., 1997; Negre-Salvayre et al., 1997), enhancement of such expression has been mainly recorded in hepatocytes in situations of metabolic

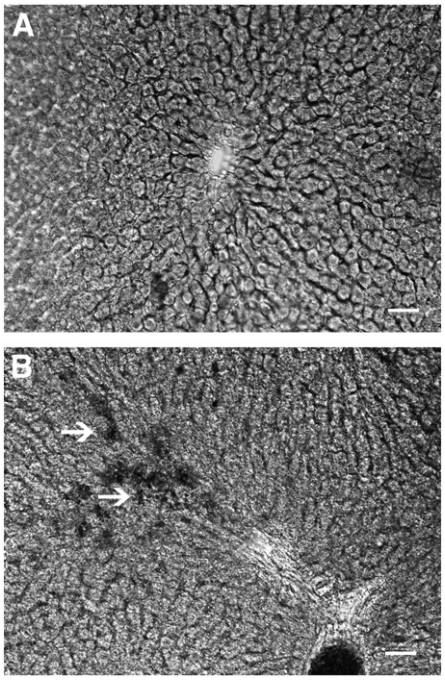

Fig. 2. Liver lipid accumulation. Photomicrographs of liver sections from C (A) and FRD (B) rats. The histological features show mixed macrovesicular and microvesicular fat deposits (white arrows), with zonal distribution (zone two). Sudan red/200. The bar represents 100 µm.

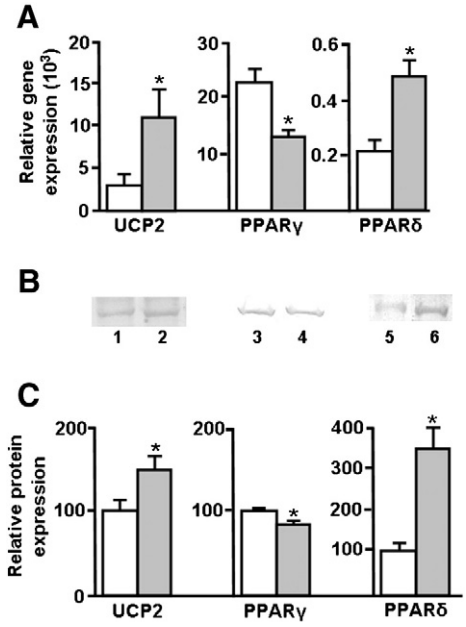

Fig. 3. FRD-induced changes in UCP2, PPARγ and PPARδ relative gene (A) and protein (B,C) expression. (B) Representative blots show the bands corresponding to UCP2, PPARγ and PPARδ protein in C (lanes 1, 3 and 5) and FRD (lanes 2, 4 and 6) rats. (C) Band intensities were measured in C (white bars) and FRD (gray bars) animals. Results are means ± SEM of 5 different experiments run in triplicate. *$P<0.05$.

stress (Nakatani et al., 2002). In our FRD rats, we recorded increased UCP2 gene and protein expression in liver homogenates.

Increased liver UCP2 mRNA expression has been reported under different circumstances, namely, in response to starvation, in obese, leptin-deficient animals, and in rodents treated with a high-fat diet (Kersten et al., 1999; Memon et al., 2000; Patsouris et al., 2006). Our data showed that the intake of a high-monosaccharide diet (FRD) is another condition able to increase such expression.

Since the changes measured in UCP2 expression were associated to an increase in glycoxidative stress markers in FRD rats (i.e., a reduction in GSH and an increase in protein carbonyl groups), we could link both changes applying the "mild" uncoupling mechanism suggested by Skulachev (1998). In this regard, the metabolic overload caused by high fructose leads to an increase in ATP synthesis with the consequent ADP depletion. This in turn inhibits the mitochondrial electron transport chain and increases ROS production. To prevent the latter effect, the high expression of UCPs limits ROS production (Arsenijevic et al., 2000; Boss et al., 2000; Diehl and Hoek, 1999; Skulachev, 1998). On the other hand, it has been proposed that UCPs play a regulatory role upon mitochondrial generation of hydrogen peroxide (Negre-Salvayre et al., 1997). Following this reasoning, UCP2 would dissipate the mitochondrial proton-motive force with the consequent decrease of ROS production (Joseph et al., 2002). Further, an elevated ROS formation has been recorded in a model of UCP2 knockout mice when exposed to a pathogen agent (Arsenijevic et al., 2000). Altogether, these data lend support to our assumption that under our experimental conditions, the increased UCP2 gene and protein expression could be part of an adaptive mechanism to the metabolic overload caused by short-term FRD administration.

PPARs have been recently identified as pivotal factors in the control of UCPs gene transcription, and PPARα and PPARγ have been shown to up regulate UCPs expression (Aubert et al., 1997; Auwerx, 1999; Shimabukuro et al., 1997). Chronic treatment of rodents with PPARα agonists increases liver UCP2 mRNA expression (Memon et al., 2000; Tsuboyama-Kasaoka et al., 1999); troglitazone (PPARγ activator) also induces UCP2 expression in cultured hepatocytes (Villarroya et al., 2007), and adenoviral-induced overexpression of PPARγ in the liver of PPARα- null mice fed a high-fat diet increased the levels of

UCP2 mRNA (Patsouris et al., 2006). On the other hand, the increase in liver UCP2 expression induced by starvation is preserved in PPARα-null animals (Kersten et al., 1999). These results suggest that PPARs can play a redundant effect upon UCP2 expression and that additional signaling mechanisms also participate in the control of such process.

In our study, we measured uneven changes in PPAR gene expression of FRD rat liver: an increase in PPARδ, a decrease in PPARγ and no changes in PPARα; changes were accompanied by a parallel increase in the expression of two genes controlled by PPARδ, FAS and GPAT, which in turn switch metabolism towards lipid synthesis. The higher triglyceride content found in the liver of these rats supports the latter assumption. It has been recently shown that PPARδ regulates metabolic homeostasis and insulin sensitivity through a unique mechanism consisting of increased fat production in the liver to consume glucose, and a counterbalancing burning of fat by the muscle to reduce lipid burden (Lee et al., 2006). The current changes recorded in lipid metabolism of FRD rats as well as data previously reported by our group (Francini et al., 2010) are consistent with that homeostatic mechanism.

We must admit, however, that despite we did not measure significant changes in PPARα gene expression in FRD rats, other authors have reported its reduction (Nagai et al., 2002; Roglans et al., 2007). Our design cannot provide a reasonable explanation for this and other apparent discrepancies. However, assuming the possible redundant metabolic effect of PPARs, we could argue that the different PPARs possibly react in different ways according to the stimuli/experimental model used. Further experiments specially designed for that purpose are needed to provide a definite answer to this question.

Conclusion

Our data show that rats fed a FRD for 3 weeks present increased UCP2 gene and protein expression, which could be part of a compensatory mechanism used by the liver to reduce ROS production in a situation of fructose overload. PPARs expression would participate actively in the regulation of UCP2 expression, and under the metabolic condition tested, PPARδ could play a key role. This knowledge would help to better understand the mechanisms involved in liver adaptation to fructose-induced glycoxidative stress and to develop appropriate prevention strategies in conditions such as obesity and T2DM.

Conflict of interest statement

There is no conflict of interest.

Acknowledgements

This study was supported by grants from CONICET and Universidad Nacional de La Plata, Argentina. The authors are grateful to Adrián Díaz for insulin assays, Adriana Di Maggio for careful manuscript editing and César E. Bianchi for technical support.

References

Alzamendi A, Giovambattista A, Raschia A, Madrid V, Gaillard RC, Rebolledo O, et al. Fructose-rich diet-induced abdominal adipose tissue endocrine dysfunction in normal male rats. Endocrine 2009;35(2):227–32.
Arsenijevic D, Onuma H, Pecqueur C, Raimbault S, Manning BS, Miroux B, et al. Disruption of the uncoupling protein-2 gene in mice reveals a role in immunity and reactive oxygen species production. Nat Genet 2000;26(4):435–9.
Aubert J, Champigny O, Saint-Marc P, Negrel R, Collins S, Ricquier D, et al. Up-regulation of UCP-2 gene expression by PPAR agonists in preadipose and adipose cells. Biochem Biophys Res Commun 1997;238(2):606–11.
Auwerx J. PPARgamma, the ultimate thrifty gene. Diabetologia 1999;42(9):1033–49.
Boss O, Hagen T, Lowell BB. Uncoupling proteins 2 and 3. Potential regulators of mitochondrial energy metabolism. Diabetes 2000;49(2):143–56.
Bradford MM. A rapid and sensitive method for the quantitation of microgram quantities of protein utilizing the principle of protein-dye binding. Anal Biochem 1976;72:248–54.
Bray GA, Nielsen SJ, Popkin BM. Consumption of high-fructose corn syrup in beverages may play a role in the epidemic of obesity. Am J Clin Nutr 2004;79(4):537–43.
Busserolles J, Zimowska W, Rock E, Rayssiguier Y, Mazur A. Rats fed a high sucrose diet have altered heart antioxidant enzyme activity and gene expression. Life Sci 2002;71(11):1303–12.
Chomczynski P, Sacchi N. Single-step method of RNA isolation by acid guanidinium thiocyanate–phenol–chloroform extraction. Anal Biochem 1987;162(1):156–9.
Diehl AM, Hoek JB. Mitochondrial uncoupling: role of uncoupling protein anion carriers and relationship to thermogenesis and weight control "the benefits of losing control". J Bioenerg Biomembr 1999;31(5):493–506.
Francini F, Castro MC, Gagliardino JJ, Massa ML. Regulation of liver glucokinase activity in rats with fructose-induced insulin resistence and impaired glucose and lipid metabolism. Can J Physiol Pharmacol 2009;87(9):702–10.
Francini F, Castro C, Schinella G, Garcia ME, Maiztegui B, Raschia MA, et al. Changes induced by a fructose-rich diet on hepatic metabolism and the antioxidant system. Life Sci 2010;86(2010):965–71.
Girard A, Madani S, Boukortt F, Cherkaoui-Maiki M, Belleville J, Prost J. Fructose-enriched diet modifies antioxidant status and lipid metabolism in spontaneously hypertensive rats. Nutrition 2006;22(7–8):758–66.
Gross LS, Li L, Ford ES, Liu S. Increased consumption of refined carbohydrates and the epidemic of type 2 diabetes in the United States: an ecologic assessment. Am J Clin Nutr 2004;79(5):774–9.
Guthrie JF, Morton JF. Food sources of added sweeteners in the diets of Americans. J Am Diet Assoc 2000;100(1):43–8.
Herbert V, Lau KS, Gottlieb CW, Bleicher SJ. Coated charcoal immunoassay of insulin. J Clin Endocrinol Metab 1965;25(19):1375–84.
Joseph JW, Koshkin V, Zhang CY, Wang J, Lowell BB, Chan CB, et al. Uncoupling protein 2 knockout mice have enhanced insulin secretory capacity after a high-fat diet. Diabetes 2002;51(11):3211–9.
Kersten S, Seydoux J, Peters JM, Gonzalez FJ, Desvergne B, Wahli W. Peroxisome proliferator-activated receptor alpha mediates the adaptive response to fasting. J Clin Invest 1999;103(11):1489–98.
King H, Aubert RE, Herman WH. Global burden of diabetes, 1995–2025: prevalence, numerical estimates, and projections. Diabetes Care 1998;21(9):1414–31.
Lange AJ, Arion WJ, Beaudet AL. Type Ib glycogen storage disease is caused by a defect in the glucose-6-phosphate translocase of the microsomal glucose-6-phosphatase system. J Biol Chem 1980;255(18):8381–4.
Larrouy D, Laharrague P, Carrera G, Viquerie-Bascands N, Levi-Meyrueis C, Fleury C, et al. Kupffer cells are a dominant site of uncoupling protein 2 expression in rat liver. Biochem Biophys Res Commun 1997;235(3):760–4.
Lee CH, Olson P, Hevener P, Mehl I, Chong LW, Olefsky JM, et al. PPARδ regulates glucose metabolism and insulin sensitivity. Proc Natl Acad Sci U S A 2006;103(9):3444–9.
Levine RL, Garland D, Oliver CN, Amici A, Climent I, Lenz AG, et al. Determination of carbonyl content in oxidatively modified proteins. Methods Enzymol 1990;186:464–78.
Linde S, Hansen B, Lermark A. Stable iodinated polypeptide hormones prepared by polyacrylamide gel electrophoresis. Anal Biochem 1980;107(1):165–76.
Malik VS, Popkin BM, Bray GA, Després JP, Willett WC, Hu FB. Sugar sweetened beverages and risk of metabolic syndrome and type 2 diabetes: a meta-analysis. Diabetes Care 2010;33(11):2477–83.
Matthews DR, Hosker JP, Rudenski AS, Naylor BA, Treacher DF, Turner RC. Homeostasis model assessment: insulin resistance and beta-cell function from fasting plasma glucose and insulin concentrations in man. Diabetologia 1985;28(7):412–9.
Memon RA, Tecott LH, Nonogaki K, Beigneux A, Moser AH, Grunfeld C, et al. Up-regulation of peroxisome proliferator-activated receptors (PPAR-alpha) and PPAR-gamma messenger ribonucleic acid expression in the liver in murine obesity: troglitazone induces expression of PPAR-gamma-responsive adipose tissue-specific genes in the liver of obese diabetic mice. Endocrinology 2000;141(11):4021–31.
Nagai Y, Nishio Y, Nakamura T, Maegawa H, Kikkawa R, Kashiwagi A. Amelioration of high fructose-induced metabolic derangements by activation of PPARalpha. Am J Physiol Endocrinol Metab 2002;282(5):E1180–90.
Nakatani T, Tsuboyama-Kasaoka N, Takahashi M, Miura S, Ezaki O. Mechanism for peroxisome proliferator-activated receptor-alpha activator-induced up-regulation of UCP2 mRNA in rodent hepatocytes. J Biol Chem 2002;277(11):9562–9.
Negre-Salvayre A, Hirtz C, Carrera G, Cazenave R, Troly M, Salvayre R, et al. A role for uncoupling protein-2 as a regulator of mitochondrial hydrogen peroxide generation. FASEB J 1997;11(10):809–15.
Patsouris D, Reddy JK, Müller M, Kersten S. Peroxisome proliferator-activated receptor alpha mediates the effects of high-fat diet on hepatic gene expression. Endocrinology 2006;147(3):1508–16.
Putnam J, Allshouse J. Food consumption prices and expenditures, 1970–97. Statistical Bulletin No. 965. Washington D.C: Economic research service, USDA; 1999.
Rebolledo OR, Marra CA, Raschia A, Rodríguez S, Gagliardino JJ. Abdominal adipose tissue: early metabolic dysfunction associated to insulin resistance and oxidative stress induced by an unbalanced diet. Horm Metab Res 2008;40(11):794–800.
Roglans N, Vilà L, Farré M, Alegret M, Sánchez RM, Vázquez-Carrera M, et al. Impairment of hepatic Stat-3 activation and reduction of PPARalpha activity in fructose-fed rats. Hepatology 2007;45(3):778–88.
Rousset S, Alves-Guerra MC, Mozo J, Miroux B, Cassard-Doulcier AM, Bouillaud F, et al. The biology of mitochondrial uncoupling proteins. Diabetes 2004;53(Suppl. 1):S130–5.
Schwartz DM, Wollins NE. A simple and rapid method to assay triacylglycerol in cells and tissues. J Lipid Res 2007;48(11):2514–20.
Sedlak J, Lindsay RH. Estimation of total, protein-bound, and nonprotein sulfhydryl groups in tissue with Ellman's reagent. Anal Biochem 1968;25(1):192–205.

Shimabukuro M, Zhou YT, Lee Y, Unger RH. Induction of uncoupling protein-2 mRNA by troglitazone in the pancreatic islets of Zucker diabetic fatty rats. Biochem Biophys Res Commun 1997;237(2):359–61.
Skulachev VP. Uncoupling: new approaches to an old problem of bioenergetics. Biochim Biophys Acta 1998;1363(2):100–24.
Thirunavukkarasu V, Nandhini ATA, Anuradha CV. Cardiac lipids and antioxidant status in high fructose rats and the effect of alpha-lipoic acid. Nutr Metab Cardiovasc Dis 2004;14(6):351–7.
Tsuboyama-Kasaoka N, Takahashi M, Kim H, Ezaki O. Up-regulation of liver uncoupling protein-2 mRNA by either fish oil feeding or fibrate administration in mice. Biochem Biophys Res Commun 1999;257(3):879–85.
Villarroya F, Iglesias R, Giralt M. PPARs in the control of uncoupling proteins gene expression. PPAR Res 2007;2007. doi:10.1155/2007/74364. Article ID 74364, 12 pages.